LA-UR- 09-05565

Title: The solubility of hydrogen and deuterium in alloyed, unalloyed and impure plutonium metal

Author(s): S Richmond,
J S Bridgewater,
J W Ward,
T A Allen

Intended for: Actinides 2009 conference proceedings in the IOP Conference Series: Materials Science and Engineering.

The solubility of hydrogen and deuterium in alloyed, unalloyed and impure plutonium metal

S Richmond, J S Bridgewater, J W Ward and T H Allen

Los Alamos National Laboratory, Los Alamos, NM, USA

E-mail: richmond@lanl.gov

Abstract. Pressure-Composition-Temperature (PCT) data are presented for the plutonium-hydrogen (Pu-H) and plutonium-deuterium (Pu-D) systems in the solubility region up to terminal solubility (precipitation of PuH_2). The heats of solution for PuH_S and PuD_S are determined from PCT data in the ranges 350-625°C for gallium alloyed Pu and 400-575°C for unalloyed Pu. The solubility of high purity plutonium alloyed with 2 at.% gallium is compared to high purity unalloyed plutonium. Significant differences are found in hydrogen solubility for unalloyed Pu versus gallium alloyed Pu. Differences in hydrogen solubility due to an apparent phase change are observable in the alloyed and unalloyed solubilities. The effect of iron impurities on Pu-Ga alloyed Pu is shown via hydrogen solubility data as preventing complete homogenization.

1. Introduction

Plutonium metal absorbs hydrogen exothermically. Unlike most other metals, plutonium does not require any removal or disruption of the oxide layer to begin rapid hydriding and the bulk metal will hydride at a prodigious rate [1] if supplied with hydrogen. The thermodynamics of the plutonium-hydrogen system has been investigated many times [2], but the plutonium-hydrogen solution ($Pu\text{-}H_S$) phase was overlooked. Since hydrogen has been shown to greatly increase corrosion of plutonium [3] and since the rate at which hydrogen enters a metal, the hydrogen permeability, has been shown to be dominated by the heat of solution [4], measuring the plutonium-hydrogen solution system also has practical value.

Hydrogen absorbs into a metal, *M*, by a process of adsorption, dissociation and dissolution into the metal [5]. At equilibrium the chemical potential of the gas, μ^g, is equal to the chemical potential of hydrogen in the metal, $\mu(H/M)$. The solution equilibrium condition is,

$$M + \frac{x}{2} H_2 \xleftrightarrow{K_S} MH_x \;, \tag{1}$$

$$\tfrac{1}{2}\mu^g = \mu(H/M) \,. \tag{2}$$

In equation (1) K_S is the equilibrium constant, also known as the Sieverts' constant, is given by:

$$K_S = \frac{H}{M} \cdot \left(\frac{p}{p_0} \right)^{-\frac{1}{2}} \quad \text{or, less formally,} \quad K_S = \frac{H}{M} \cdot \sqrt{p} \qquad (3)$$

Equation (2), also known as Sievert's law [5,6] shows that at equilibrium H/M varies proportionally with the square root of the pressure, p, indicating that atomic hydrogen, H, rather than H_2, is in solution in the metal. Equation (2) is generally valid for a dilute solution, less than a few percent H/M, and low pressures (<100 ATM) [4]. The value of p_0 is customarily one atmosphere (1 ATM) for historical consistency. The Sieverts' constant varies in an Arrhenius fashion, so a plot of $\ln(K_S)$ versus $1/T$ has a line whose slope is the heat of solution, ΔH_S, of hydrogen in the metal, divided by the gas constant. Consequently,

$$K_S = K_0 \cdot e^{-\frac{\Delta H_S}{RT}} \cdot e^{\frac{\Delta S^{nc}}{R}} \qquad (4)$$

describes the solubility of hydrogen in a metal as a function of the heat and entropy (non-configurational) of solution, ΔH_S and ΔS^{nc}, and absolute temperature, T. R is the gas constant. If K_0 is known and the $\ln(K_S/K_0)$ is plotted versus $1/T$ then intercept of the line, where $1/T$ approaches 0 ($T=\infty$), is the non-configurational entropy of solution, ΔS^{nc}, divided by the gas constant, R.

If the heats of solution, ΔH_S, and non-configurational entropy of solution, ΔS^{nc}, are known for each allotropic solid phase and the liquid phase, then the solvus line of the Pu-H phase diagram can be established for all temperatures and compositions where the free energy of solution, ΔG_S, is equal to the free energy of formation of the dihydride (PuH_2), ΔG_F. In other words, at the solvus line:

$$\Delta G_S = \Delta G_F = \Delta H_S - T \cdot \Delta S^{nc} = \Delta H_F - T \cdot \Delta S_F \qquad (5)$$

The solvus line is the point of maximum hydrogen in solution in equilibrium with the dihydride. At this point, at a given temperature, the addition of any hydrogen to the metal results in precipitation of the dihydride because it is a saturated solution. It is plutonium metal in this condition that Haschke et . al. [ref] have shown is extremely susceptible to corrosion. This experiment investigates the nature of hydrogen incorporation from hydrogen free to saturated solution for alloyed and unalloyed Pu.

2. Experiment

The solubility of H in Pu was measured using a Sieverts type apparatus. In the Sieverts apparatus a vessel which contains the sample (~1 to 2 g) was held at constant temperature and measured quantities of gas were equilibrated either to or from the sample via a second vessel of known volume. The equilibrium pressure of the gas during each addition or removal of gas was recorded. Between equilibrations the sample in the vessel was isolated from the equilibrium vessel with a valve and the equilibrium vessel was either evacuated in the case of desorption or filled to a desired pressure in the case of absorption. Based on the ideal gas law, the equilibrium vessel pressure, temperature and volume were used to determine the amount of hydrogen in the sample at each point.

The data obtained in this way is placed into a pressure-composition-temperature plot or PCT. A series of PCT isotherms were produced in this fashion for pure Pu and Pu-2 at.%-Ga using pure hydrogen and deuterium. The accuracy of the temperature measurement is ±2°C, and pressure ±0.1% of full scale. A 1 Torr and 100 mTorr capacitance manometer were used. The accuracy of the volumes used is ±4%. Sample masses are a measured to within 5 mg.

3. Results and discussion

3.1. The H_2 absorption PCT isotherms for unalloyed Pu in the temperature range 400-825°C.

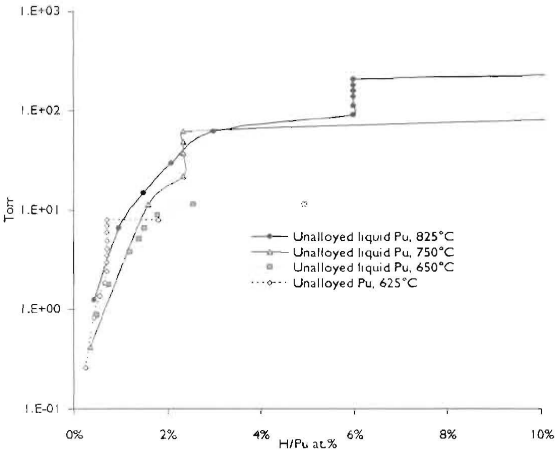

Figure 1. H_2 absorption isotherm for unalloyed liquid Pu.

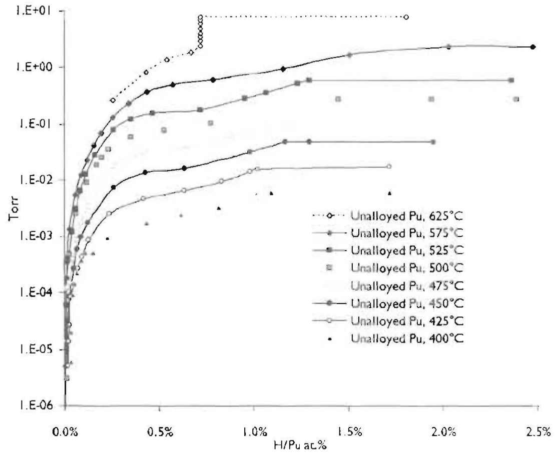

Figure 2. H_2 PCT absorption isotherms for solid unalloyed Pu.

The H_2 absorption PCT isotherms for unalloyed Pu are shown in figures 1 and 2. PuH_2 is evidently a solid with a melting point above 825°C because the pressure increases appreciably at the terminal solubility of H in liquid Pu with no compositional change (H/Pu is constant), due to the heat of fusion of PuH_2. The same feature is evident at 625°C, 15°C below the melting point of Pu, indicating depression of the Pu melting point. The 625°C sample did not appear to be melted but did stick to its sample holder, so that sample appears to have experienced partial melting. The heat of fusion of PuH_2 is estimated from this data to be 8679 J/mol. (~0.1eV). The same 625°C isotherm is included on both the liquid and solid plots. The solid unalloyed Pu isotherms all display an inflection at about 0.6-0.7 at.% H/Pu. This inflection was first noted by Allen [2] in 1991 but could not be explained.

3.2. The H_2 absorption PCT isotherms for Pu-2 at.%-Ga in the temperature range 350-625°C.

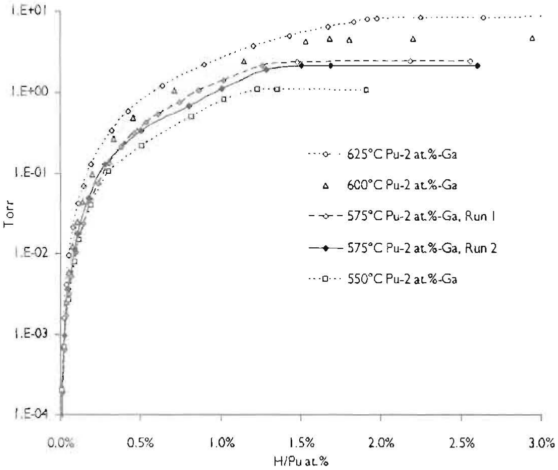

Figure 3. H_2 PCT absorption isotherms for solid Pu-2 at.%-Ga from 550-625°C.

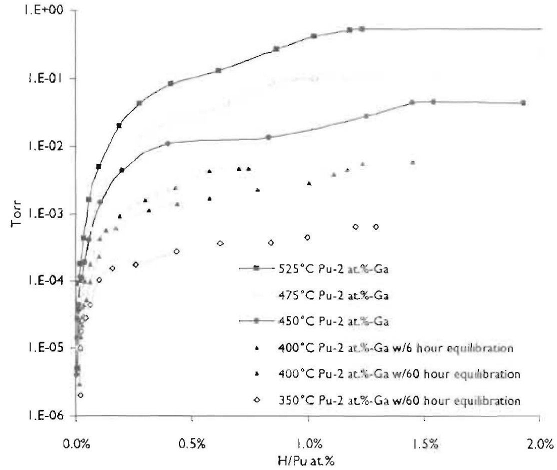

Figure 4. H_2 PCT absorption isotherms for solid Pu-2 at.%-Ga from 350-525°C.

The inflection observed in unalloyed isotherms is also significant below 550°C in Pu-2 at.%-Ga H_2 isotherms (Figure 4).

3.3. The D_2 absorption PCT isotherms for Pu-2 at.%-Ga in the temperature range 400-625°C.

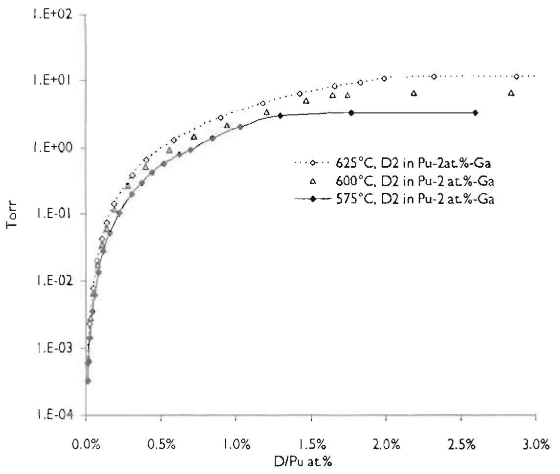

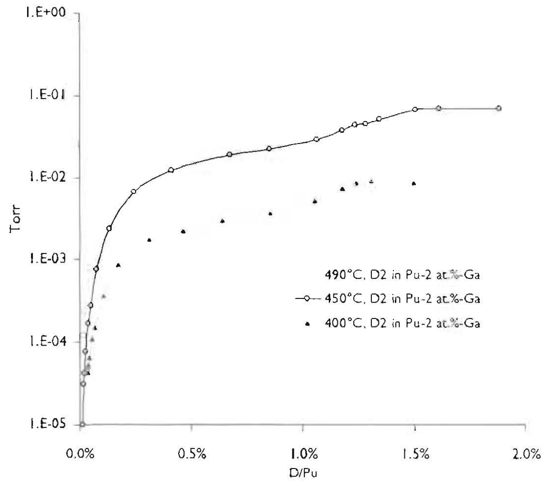

Figure 5. D_2 PCT absorption isotherms for solid Pu-2 at.%-Ga from 575-625°C.

Figure 6. D_2 PCT absorption isotherms for solid Pu-2 at.%-Ga from 400-490°C.

3.4. Interpretation of the isotherm data.

The data shown in figures 1-6 is plotted as $p^{1/2}$ versus composition and a Sieverts' constant is determined. Figures 7 and 8 show the Sieverts' plots for hydrogen in Pu-2 at.%-Ga.

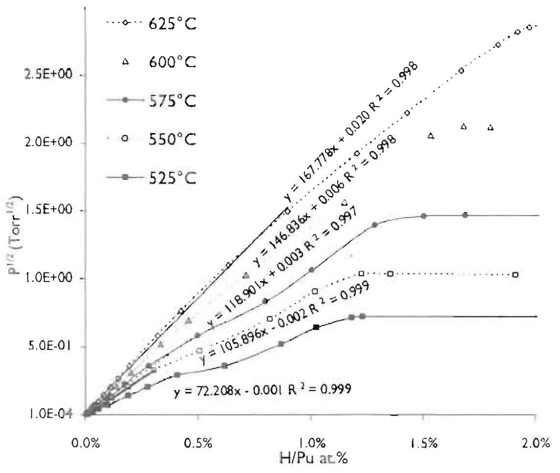

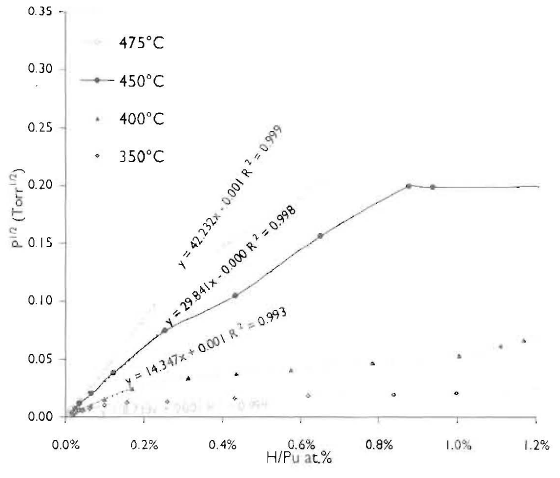

Figure 7. Sieverts' Plot for H_2 in Pu-2 at.%-Ga from 575-625°C showing linear fit.

Figure 8. Sieverts' plot for H_2 in Pu-2 at.%-Ga from 350-475°C showing linear fit.

In the linear region of each data set, a fit is obtained. The fit is only applied in the dilute solution region where linear square root behaviour conforms to Sieverts' Law (2). The linear fit is the equation of a line where $y=mx+b$ and b is very nearly zero in each case. So that the Sieverts' constant is taken from these plots as $K_S=1/m$, as in (2) but neglecting p_0. The Sieverts' constants were similarly obtained for H_2 in unalloyed Pu and for D_2 in Pu-2 at.%-Ga. The $\ln(K_S)$ vs. $1/T$ of the data obtained are shown in Figure 9.

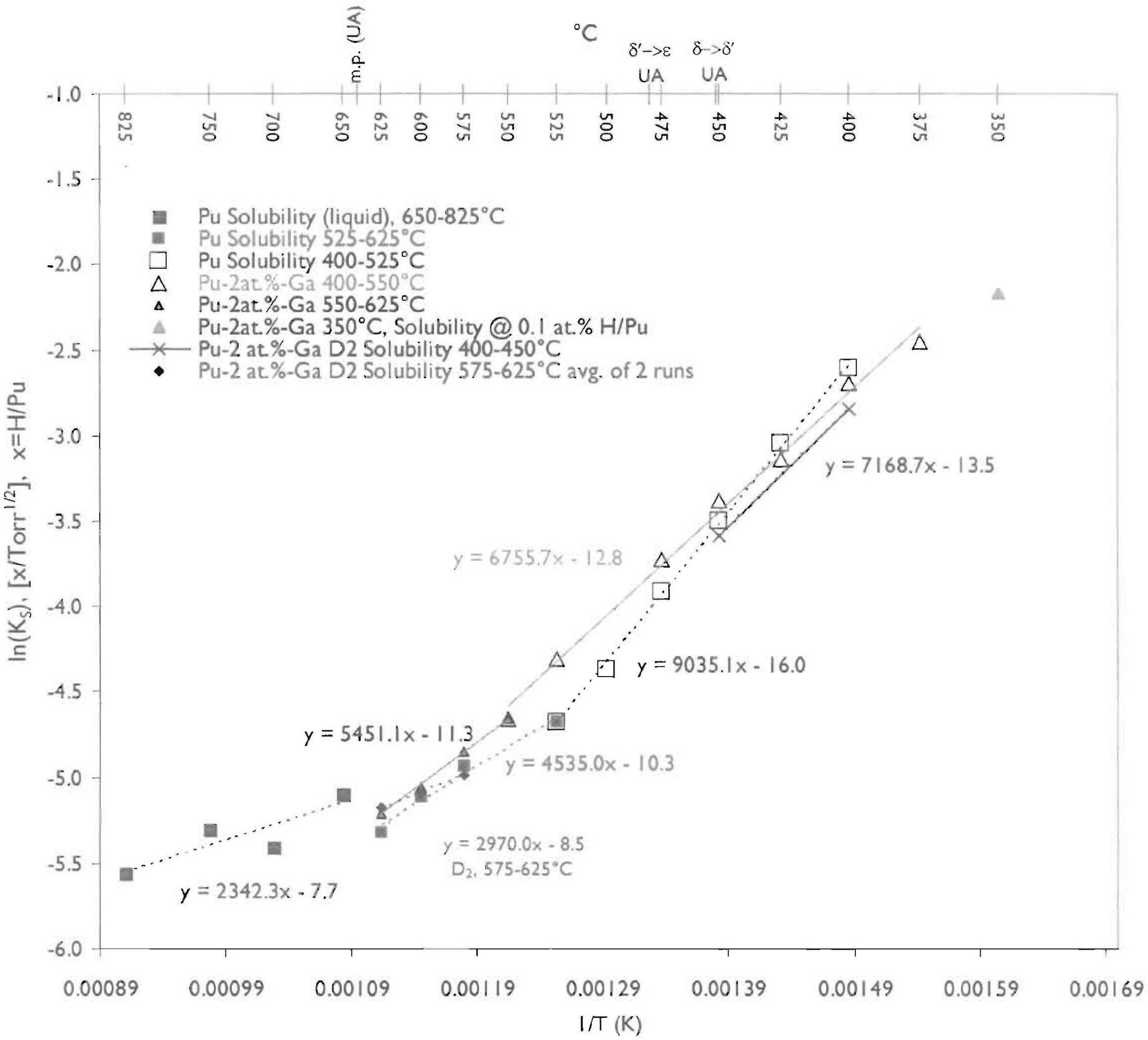

Figure 9. Arrhenius plot of the natural log of the Sieverts' constants, K_S, for H_2 and D_2 in Pu-2 at.%-Ga and H_2 in unalloyed (UA) Pu. The unalloyed Pu melting point (m.p.), δ->δ′ and δ′->ε transition temperatures are noted on the upper scale. The Pu-2 at.%-Ga δ->(δ + ε) occurs at ~476°C.

Each set of data has a best fit line of the form $y=mx+b$. Multiplying the slope (m) of a given fit by the gas constant (R=8.314 J·mol^{-1}·K^{-1}) gives the heat of solution:

$$\Delta H_S = -R \cdot \frac{\partial \ln(K_S)}{\partial \frac{1}{T}}. \tag{6}$$

The energies obtained from from each fit shown in figure 9 are listed in Table 1. Wipf [4] has shown that enthalpies and entropies of solution can also be determined from the pressure isotherm data at constant composition and very dilute solution ($x<<r$), where:

$$\Delta H_S = \tfrac{1}{2} \cdot R \cdot \left. \frac{\partial \ln(p/p_0)}{\partial \frac{1}{T}} \right|_{X=\text{const.}} , \tag{7}$$

$$\Delta S^{nc} = R \cdot \ln(\tfrac{x}{r}) - \tfrac{1}{2} \cdot R \cdot T \cdot \left. \frac{\partial \ln(p/p_0)}{\partial T} \right|_{X=\text{const.}} . \tag{8}$$

The value of r in equation (6) is the number of interstitial sites per Pu atom and x is the composition (H/Pu). The entropies of solution in Table 1 were determined using (6) on the data of figures 1-6. Since the value of r is unknown, a plot of $\frac{1}{2} \cdot R \cdot T \cdot \ln(p/p0)$ versus T for a fixed value of x was used to get a line whose slope is ΔS^{nc} for a fixed concentration (x) over the temperature ranges associated with each plot in Figure 9. The non-configurational entropies determined in this manner for the concentrations associated with the solubility values in Figure 9 are also shown in Table 1.

Table 1. Heats of solution and non-configurational entropies of solution based on Figure 9.

	ΔH_S ($J \cdot mol^{-1}$)	ΔH_S (eV)	ΔS^{nc} ($J \cdot mol^{-1} \cdot K^{-1}$)	$\Delta S^{nc} \cdot k_B^{-1}$ [a]
liquid Pu (>639.5°C)	-19473	-0.20	05.5	0.7
Pu, 525-625°C @ H/Pu=0.25 at.%	-37704	-0.39	07.5	0.9
Pu, 400-525°C @ H/Pu=0.2 at. %	-75118	-0.78	54.0	6.5
H in Pu-2 at.%-Ga 550-625°C	-45320	-0.47	21.0	2.5
H in Pu-2 at.%-Ga 400-550°C	-56167	-0.58	49.0	5.9
D in Pu-2 at %-Ga 575-625°C	-24693	-0.26		
D in Pu-2 at %-Ga 400-450°C	-59601	-0.62		

[a] k_B is the Boltzmann constant in $eV \cdot K^{-1}$ ($8.617e\text{-}5\ eV \cdot K^{-1}$)

Notably absent in Figure 9 are inflections in the solubility at the δ->ϵ and δ->δ'->ϵ transition temperature regions for alloyed (500-525°C) and unalloyed (451-476°C) Pu respectively. δ-Pu has a face centered cubic (fcc) lattice structure with one octahedral and two tetrahedral interstitial sites per Pu atom while ϵ-Pu has a body centered cubic (bcc) lattice structure with three octahedral and six tetrahedral interstitial sites per Pu atom. Consequently the bcc structure is more soluble to hydrogen than the fcc structure. X-ray data is needed to determine why a change in solubility was not observed in these temperature ranges, but presently this capability is unavailable under these conditions for Pu.

3.4.1. *Departure from ideal solution behaviour.* The data obtained and summarized by figure 9 are only valid at dilute solution conditions. In figure 8 it can be seen that the linear portion of the $P^{1/2}$ vs. H/Pu plot is limited to very low concentrations, for example < 0.2 at.% H/Pu for the 400°C data. Beyond the Sievert's region ($P^{1/2} \propto H/M$) the metal becomes increasingly soluble to hydrogen with increasing hydrogen content. This tendency is attributed to attractive H-H interactions [5] and is observed in many metals. However, this tendency increases much more rapidly in Pu than in other metals. The region of extended solubility has varying enthalpy and entropy, which are greater than the Sievert's region but less than the enthalpy and entropy for formation of PuH_2. The region of extended solubility is most significant below ~450°C where it is the majority of the solution region. Equilibration times in this region are about 100 times slower than in the Sieverts region or at the plateau, typically 10-15 hours vs. 20 minutes. Very slow equilibration times below 450°C were also noted by Mulford and Sturdy [2] in their Pu hydriding studies.

3.5. The solubility of hydrogen in impure Pu metal.

Many hydrogen solubility measurements of Pu samples were conducted, but two alloy compositions produced unusual results, one with Fe at a level just above the solid solution limit and another with a very low Ga content (500 wppm). The isotherms are shown in Figures 10 and 11.

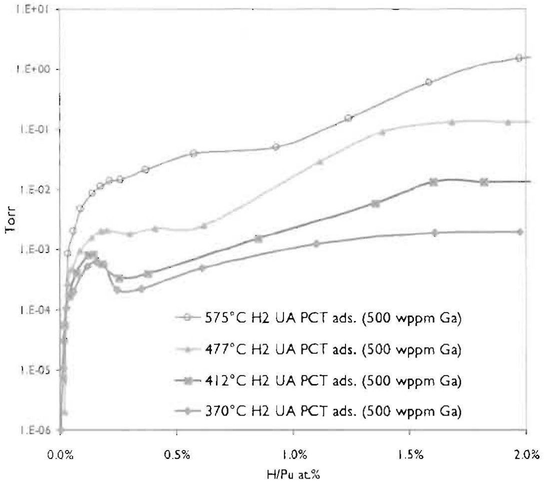

Figure 10. H_2 PCT absorption isotherms for low Ga Pu.

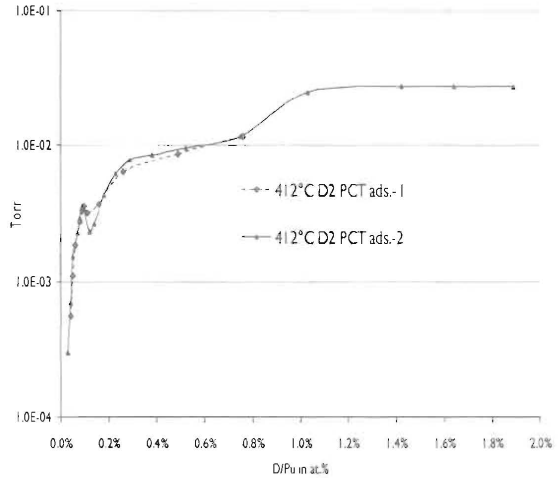

Figure 11. D_2 PCT absorption isotherms for Pu-2 at.%-Ga containing Fe impurities.

The data in Figure 10 shows that at 370-412°C as hydrogen was dissolved into the δ-phase Pu the pressure at first increased as expected, but at about 0.2 at.% H/Pu, adding H resulted in a decrease in the equilibrium pressure until about 0.4 at.% H/Pu. This means the free energy was at first decreasing but subsequently increased and finally increased again until the two phase region (plateau) was reached. The pressure reversal effect diminished as temperature was increased. Figure 11 is a plot of two equilibrium isotherms for Pu-2 at.%-Ga with Fe impurities just above the solubility limit for Fe in Pu (~0.15 at.%). The data is qualitatively similar to that in Figure 10, however the points in Figure 11 required only about 15 minutes to equilibrate vs. 15 hours for the points in Figure 10. Data was taken for Pu-2 at.%-Ga with Fe impurities from 400-625°C and it was found that equilibration times were always very short in the iron bearing samples, but that the isotherms were otherwise identical to Pu-2at.%-Ga without Fe. Only the 412°C Pu sample with Fe impurities displayed the pressure/free energy inflection. Data for the Fe impure material was taken a second time to verify the presence of the inflection and measure it more precisely. It is not known why the pressure inflections occurred, however the fact that they did occur means the chemical potential, $\mu(H/M)$, of solution has been lowered. In Figures 10 and 11, the 412°C isotherms can be bisected at single pressure and consequently a single $\mu(H/M)$ such that $\mu(x_1) = \mu(x_2) = \mu(x_3)$ .This is characteristic of spinodal decomposition, unfortunately x-ray data for Pu samples under these conditions is not presently available to confirm this definitively.

A final interesting attribute of the Fe bearing samples is that when much larger samples were loaded with hydrogen then cooled while maintaining the sample isothermal, and subsequently cutting the samples into smaller subsamples, that hydrogen content in the subsamples varied considerably (10X). This tendency was not observed in any other sample compositions.

4. Conclusions

The solubility region of the plutonium-hydrogen system has now been measured for temperatures from 400-825°C. The enthalpies and entropies of solution for H in Pu are similar to other group 3 metals whose enthalpies range from -0.77 to -0.95 eV [4, 5] and whose entropies are very small [5]. The phase boundary between solution and saturated solution was found to be near 1-2 at.% H over a wide temperature range (320-625°C). The possibility of spinodal decomposition is supported by the 370-412°C isotherms of Figures 10 and 11 and also the 400°C isotherm of Figure 2, indicating the direction for future study.

References

[1] Ward J W, Haschke J M 1994 *Handbook on the Physics and Chemistry of Rare Earths vol 18 (Chapter 123 COMPARISON OF 4f AND 5f ELEMENT HYDRIDE PROPERTIES)* ed K A Gschneider L Eyring G R Choppin and G H Lander (Amsterdam:Elsevier) p327

[2] Mulford R N R, Sturdy G E 1955 *J. Am. Chem. Soc.* **77** 3449-3452

Ward J W 1985 *Handbook on the Physics and Chemistry of The Actinides vol. 3 (Properties and Comparitive Trends in Actinide-Hydrogen Systems)* ed A J Freeman and C Keller (North-Holland: Elsevier) p1

Colmenares C, Alexander C 1975 *Lawrence Livermore National laboratory Report UCID-16799 Heat of formation of plutonium hydrides* (Livermore CA USA: Lawrence Livermore Laboratory)

Allen T H 1991 *The solubility of hydrogen in plutonium in the temperature range 475 to 825 degrees centigrade* M.S. Chemistry University of Colorado, Denver

[3] Haschke J M, Allen T H, Morales L A 2000 *Surface and corrosion chemistry of plutonium (Los Alamos Science 26 vol. 1)* pp252-273 (Los Alamos NM USA: Los Alamos National Laboratory)

[4] Wipf H H, 2001 Solubility and diffusion of hydrogen in pure metals and alloys *Physica Scripta* **T94** 43-51

[5] Fukai Y 1993 *The Metal-Hydrogen System: Basic Bulk Properties* (Berlin:Springer)

[6] Mueller W M, Blackledge J P, Libowitz G G 1968 *Metal Hydrides* (New York and London: Academic Press)